## Supplemental Information

# Impact of Backbone Rigidity on the Thermomechanical Properties of Semiconducting Polymers with Conjugation Break Spacers

Luke A. Galuska[α], William W. McNutt[β], Zhiyuan Qian[α], Song Zhang[α], Daniel W. Weller[α], Sujata Dhakal[α], Eric R. King[α], Sarah E. Morgan[α], Jason D. Azoulay[α], Jianguo Mei[β]*, Xiaodan Gu[α]*

[α]School of Polymer Science and Engineering, The University of Southern Mississippi, Hattiesburg, MS 39406, USA

[β]Department of Chemistry, Purdue University, West Lafayette, IN 47907, USA

Email: xiaodan.gu@usm.edu

Email: jgmei@purdue.edu

Downloaded from pubs.acs.org/mamobx/article-supplement/508282/pdf/ma0c00889_si_001/ by PURDUE UNIV user on 28 October 2026

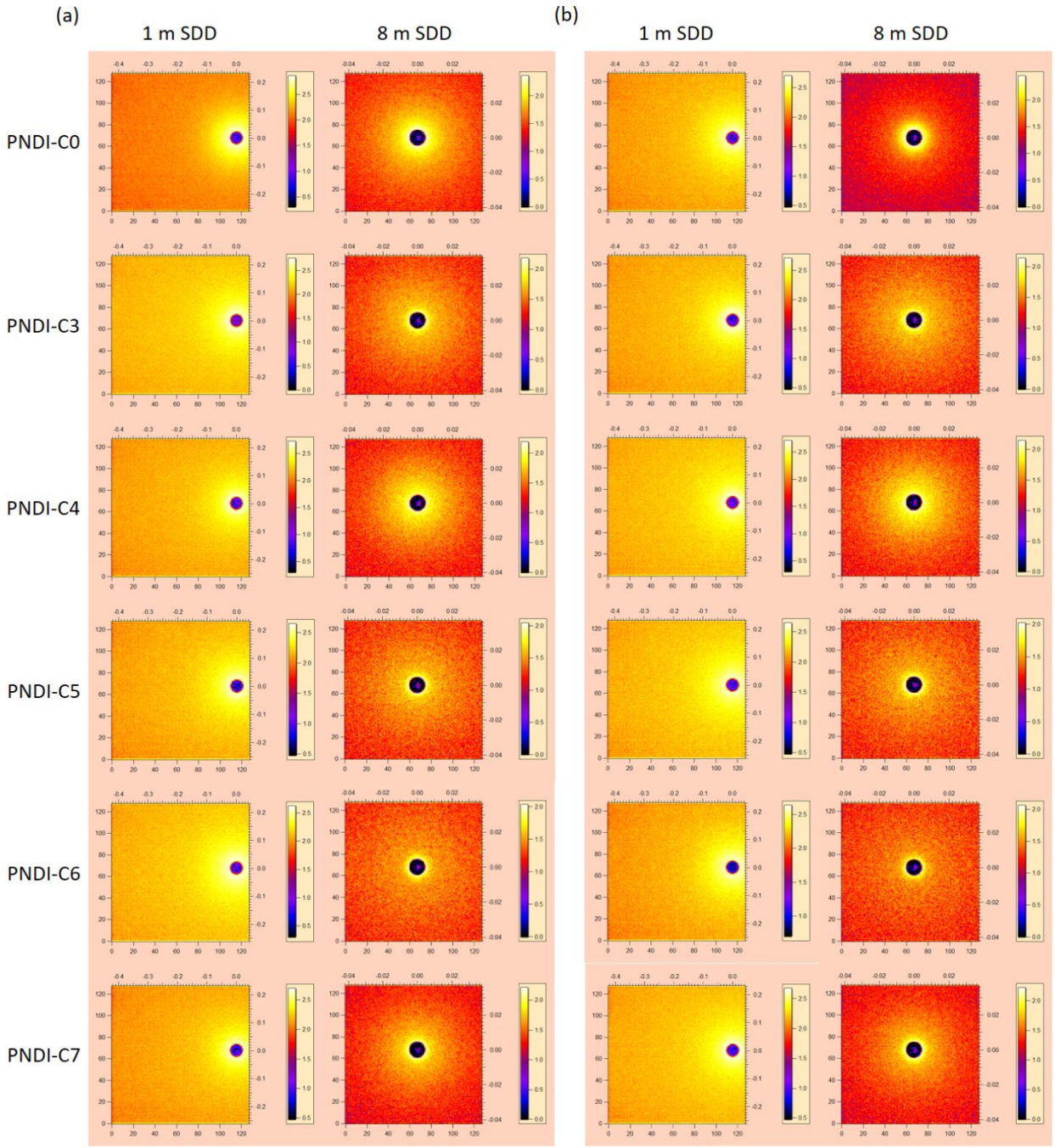


Figure S1: 2D images from solution SANS of PNDI-Cx polymers at (a) 25 ˚C and (b) 85 ˚C for sample to detector distances of 1 m and 8 m.

Downloaded from pubs.acs.org/mamobx/article-supplement/508282/pdf/ma0c00889_si_001/ by PURDUE UNIV user on 28 October 2026

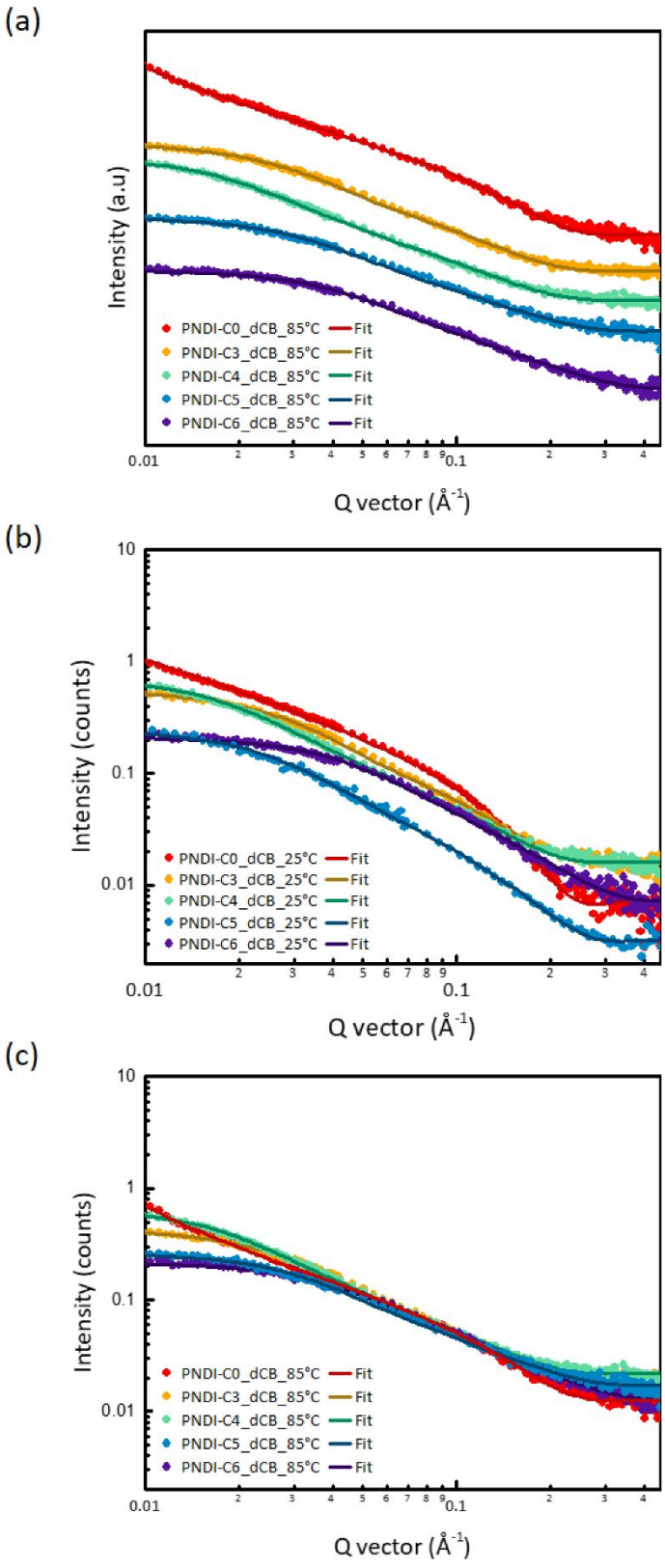


Figure S2: a) 1D scattering profile obtained at 85 ˚C in deuterated chlorobenzene b-c) SANS scattering profile at 25 and 85 ˚C with absolute intensity.



Downloaded from pubs.acs.org/mamobx/article-supplement/508282/pdf/ma0c00889_si_001/ by PURDUE UNIV user on 28 October 2026

Table S1: SANS fitting parameters and goodness of fitting obtained from SasView modeling

| | Contour length (Å) | Kuhn length (Å) | Radius (Å) | X2 (Goodness of fitting) |
|---|---|---|---|---|
| **NDI_C0 (25C)** | 476 | 521 | 14 | 4 |
| **NDI_C0 (85C)** | 310 | 196 | 12 | 2 |
| **NDI_C3 (25C)** | 271 | 85 | 13 | 4 |
| **NDI_C3 (85C)** | 276 | 84 | 13 | 2 |
| **NDI_C4 (25C)** | 447 | 86 | 13 | 2 |
| **NDI_C4 (85C)** | 449 | 88 | 13 | 2 |
| **NDI_C5 (25C)** | 221 | 86 | 10 | 2 |
| **NDI_C5 (85C)** | 233 | 58 | 10 | 2 |
| **NDI_C6 (25C)** | 180 | 36 | 9 | 2 |
| **NDI_C6 (85C)** | 180 | 45 | 8 | 2 |

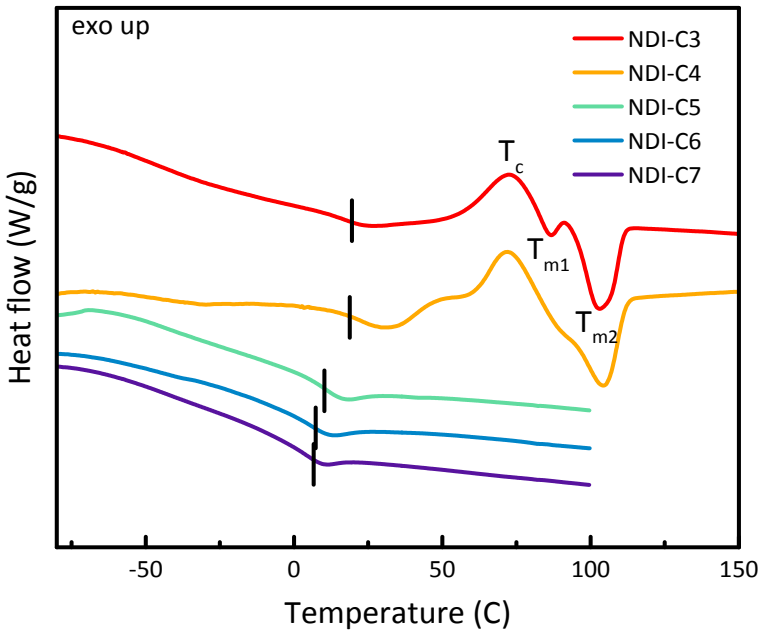


Figure S3: DSC thermogram of 2nd heat cycle for polymers C3-C7.



Downloaded from pubs.acs.org/mamobx/article-supplement/508282/pdf/ma0c00889_si_001/ by PURDUE UNIV user on 28 October 2026

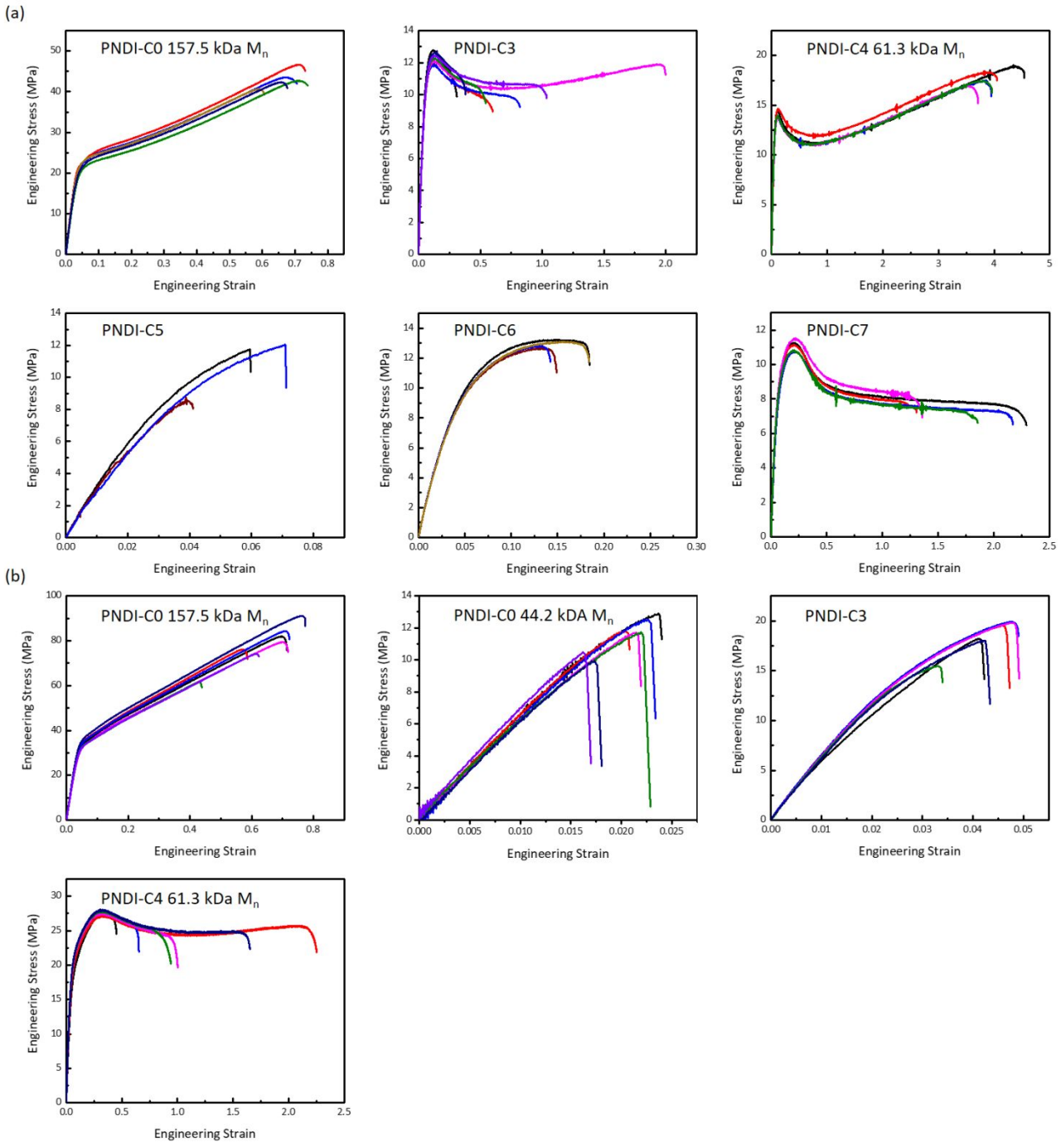


Figure S4: Raw tensile data (a) post two-day isotherm at room temperature under nitrogen atmosphere, (b) post two day annealing at 30 °C undercooling under nitrogen atmosphere (PNDI-C0 was annealed at 200 °C for eight hours)

Downloaded from pubs.acs.org/mamobx/article-supplement/508282/pdf/ma0c00889_si_001/ by PURDUE UNIV user on 28 October 2026

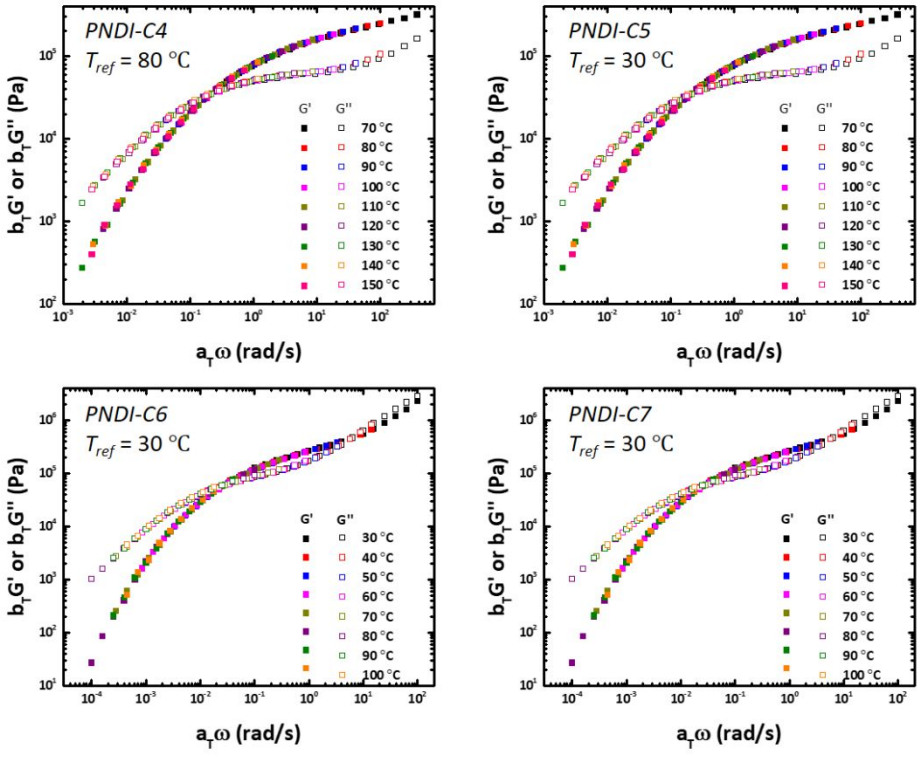


Figure S5: Master curves of PNDI-C4-7 obtained from oscillating melt shear rheology

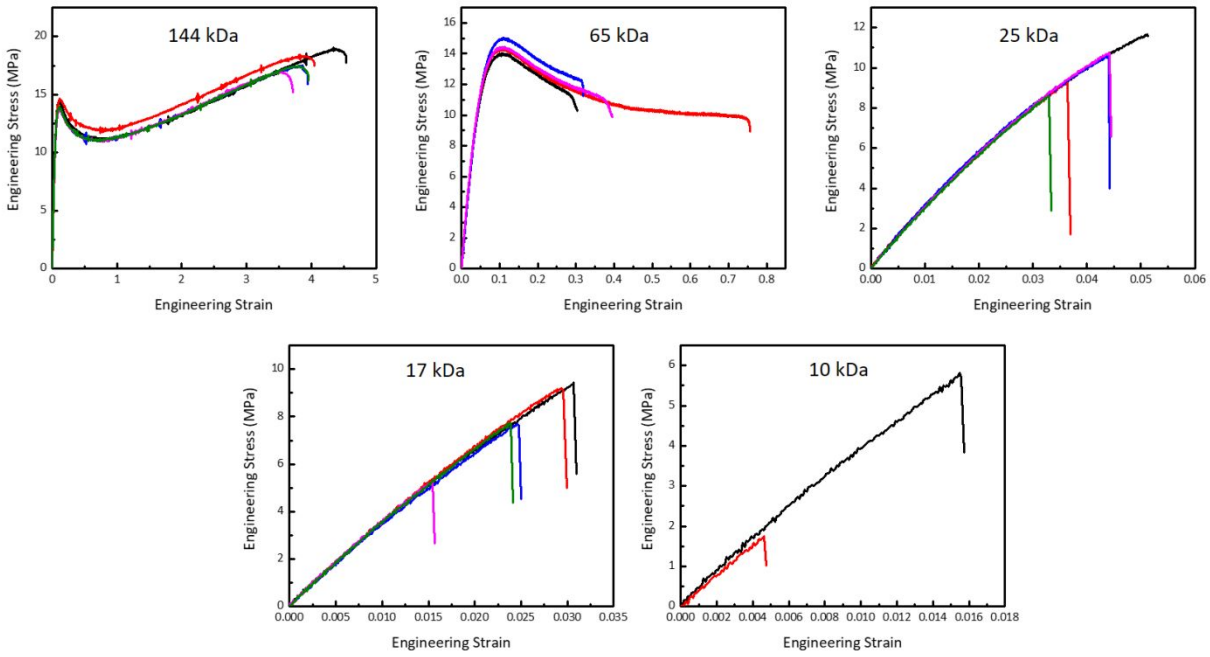


Figure S6: Raw PNDI-C4 molecular weight dependent tensile data post two-day isotherm at room temperature under nitrogen atmosphere



Downloaded from pubs.acs.org/macrobx/article-supplement/508282/pdf/ma0c00889_si_001/ by PURDUE UNIV user on 28 October 2026

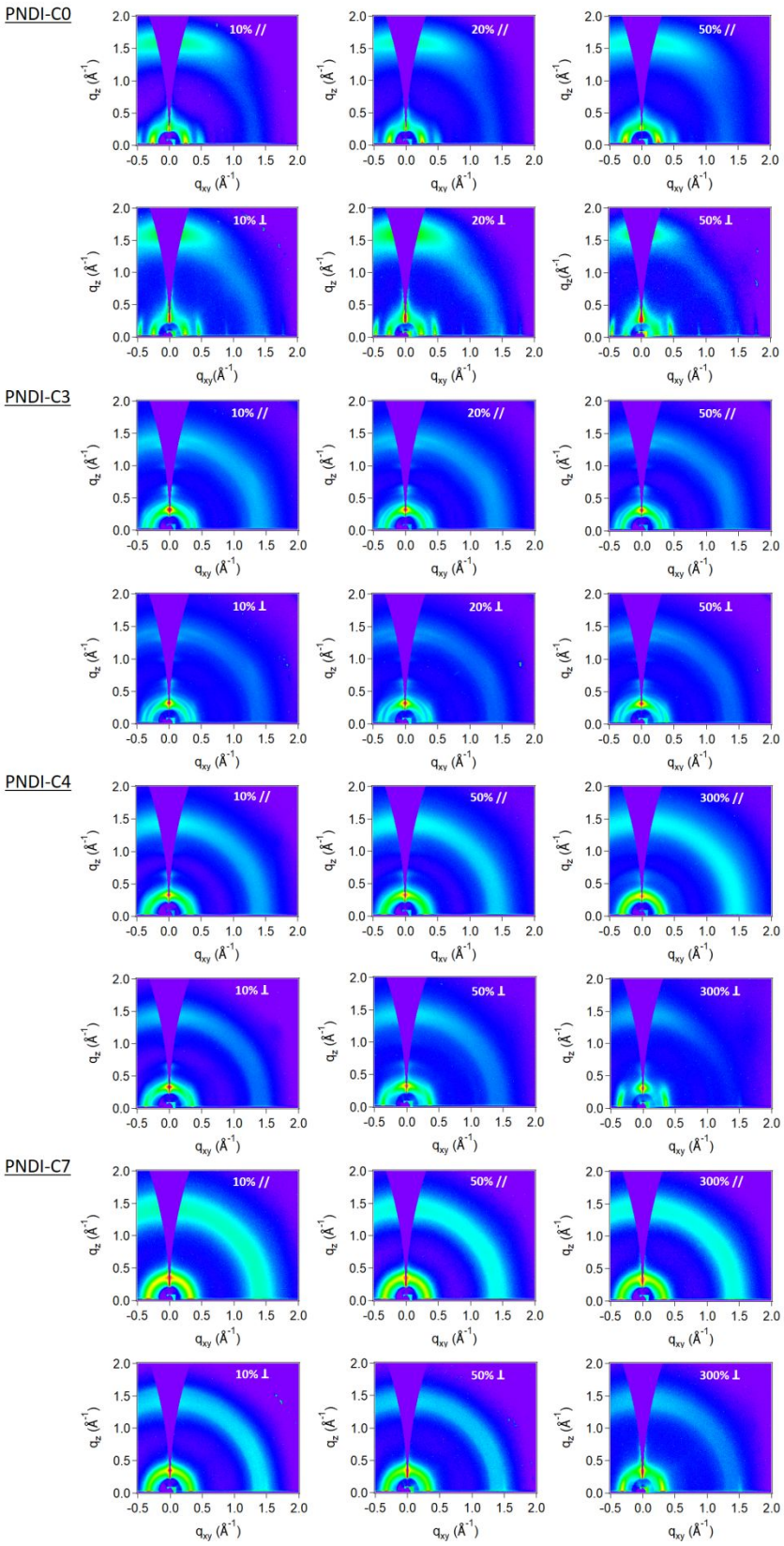


Figure S7: 2D GIWAXS scattering profiles of PNDI-C0, PNDI-C3, PNDI-C4, and PNDI-C7 under tensile strain for both parallel and perpendicular exposures relative to strain direction.



Downloaded from pubs.acs.org/mamobx/article-supplement/508282/pdf/ma0c00889_si_001/ by PURDUE UNIV user on 28 October 2026

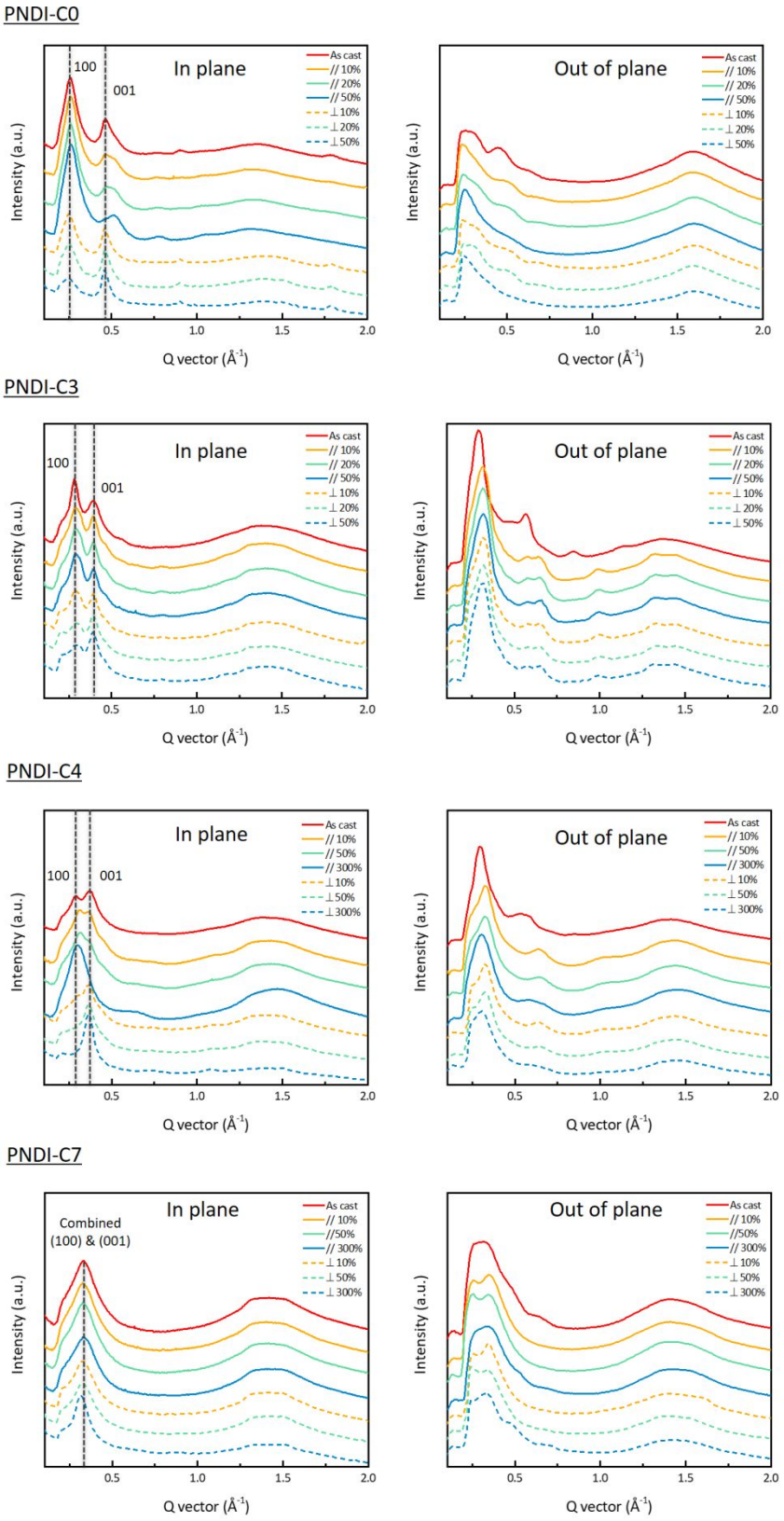


Figure S8: 1D in-plane and out of plane GIWAXS scattering profiles of PNDI-C0, PNDI-C3, PNDI-C4, and PNDI-C7 under tensile strain for both parallel and perpendicular exposures relative to strain direction.



Downloaded from pubs.acs.org/mamobx/article-supplement/508282/pdf/ma0c00889_si_001/ by PURDUE UNIV user on 28 October 2026

Table S2: Fitting results for in-plane 1D GIWAXS profiles

| | q (Å$^{-1}$) [100] | q (Å$^{-1}$) [001] | q (Å$^{-1}$) [010] | D-spacing (Å) [100] | D-spacing (Å) [001] | D-spacing (Å) [001] |
|---|---|---|---|---|---|---|
| NDI-C0 | 0.258 | 0.470 | 1.791 | 24.329 | 13.358 | 3.509 |
| NDI-C3 | 0.284 | 0.395 | NA | 22.155 | 15.919 | NA |
| NDI-C4 | 0.289 | 0.371 | NA | 21.734 | 16.939 | NA |
| NDI-C5 | 0.301 | 0.355 | 1.551 | 20.847 | 17.680 | 4.051 |
| NDI-C6 | 0.337 | | 1.454 | 18.628 | | 4.321 |
| NDI-C7 | 0.332 | | 1.439 | 18.927 | | 4.365 |

Table S3: Fitting results for in-plane 1D GIWAXS profiles post tensile strain

| | Parallel Exposure | | | | Perpendicular Exposure | | | |
|---|---|---|---|---|---|---|---|---|
| | q (Å$^{-1}$) [100] | q (Å$^{-1}$) [001] | D-spacing (Å) [100] | D-spacing (Å) [001] | q (Å$^{-1}$) [100] | q (Å$^{-1}$) [001] | D-spacing (Å) [100] | D-spacing (Å) [001] |
| **NDI-C0** | 0.258 | 0.470 | 24.329 | 13.358 | 0.258 | 0.470 | 24.329 | 13.358 |
| **10%** | 0.261 | 0.485 | 24.034 | 12.948 | 0.252 | 0.465 | 24.969 | 13.525 |
| **20%** | 0.261 | 0.499 | 24.086 | 12.589 | 0.252 | 0.465 | 24.948 | 13.499 |
| **50%** | 0.263 | 0.511 | 23.862 | 12.290 | 0.251 | 0.462 | 25.043 | 13.612 |
| **NDI-C3** | 0.284 | 0.395 | 22.155 | 15.919 | 0.284 | 0.395 | 22.155 | 15.919 |
| **10%** | 0.293 | 0.394 | 21.425 | 15.947 | 0.292 | 0.394 | 21.492 | 15.945 |
| **20%** | 0.295 | 0.394 | 21.292 | 15.935 | 0.294 | 0.394 | 21.387 | 15.967 |
| **50%** | 0.296 | 0.395 | 21.257 | 15.916 | 0.294 | 0.441 | 21.360 | 14.235 |
| **NDI-C4** | 0.289 | 0.371 | 21.734 | 16.939 | 0.289 | 0.371 | 21.734 | 16.939 |
| **10%** | 0.312 | 0.368 | 20.135 | 17.080 | 0.301 | 0.364 | 20.888 | 17.253 |
| **50%** | 0.316 | 0.370 | 19.855 | 16.983 | NA | 0.368 | NA | 17.087 |
| **300%** | 0.304 | NA | 20.702 | NA | NA | 0.366 | NA | 17.184 |
| **NDI-C5** | 0.301 | 0.355 | 20.847 | 17.680 | 0.301 | 0.355 | 20.847 | 17.680 |
| **NDI-C6** | 0.337 | | 18.628 | | 0.337 | | 18.628 | |
| **NDI-C7** | 0.332 | | 18.927 | | 0.332 | | 18.927 | |
| **10%** | 0.330 | | 19.023 | | 0.328 | | 19.147 | |
| **50%** | 0.331 | | 18.959 | | 0.328 | | 19.180 | |
| **300%** | 0.334 | | 18.821 | | 0.318 | | 19.745 | |

Downloaded from pubs.acs.org/mamobx/article-supplement/508282/pdf/ma0c00889_si_001/ by PURDUE UNIV user on 28 October 2026

Table S4: Circle gathering analysis of (100) peak for transmission WAXS of PNDI-C4 under tensile strain

| Strain | Q vector | D-spacing | FWHM | Area | Normalized area |
|---|---|---|---|---|---|
| 0% | 0.304 | 20.691 | 0.068 | 0.419 | 0.419 |
| 10% | 0.304 | 20.664 | 0.071 | 0.457 | 0.470 |
| 50% | 0.306 | 20.51 | 0.083 | 0.350 | 0.412 |
| 150% | 0.299 | 21.048 | 0.090 | 0.323 | 0.492 |
| 300% | 0.314 | 19.983 | 0.106 | 0.363 | 0.583 |

Table S5: Circle gathering analysis of (001) peak for transmission WAXS of PNDI-C4 under tensile strain

| Strain | Q vector | D-spacing | FWHM | Area | Normalized area |
|---|---|---|---|---|---|
| 0% | 0.367 | 17.105 | 0.077 | 0.601 | 0.601 |
| 10% | 0.366 | 17.148 | 0.076 | 0.578 | 0.595 |
| 50% | 0.366 | 17.163 | 0.069 | 0.528 | 0.621 |
| 150% | 0.369 | 17.032 | 0.063 | 0.554 | 0.846 |
| 300% | 0.369 | 17.031 | 0.049 | 0.400 | 0.642 |

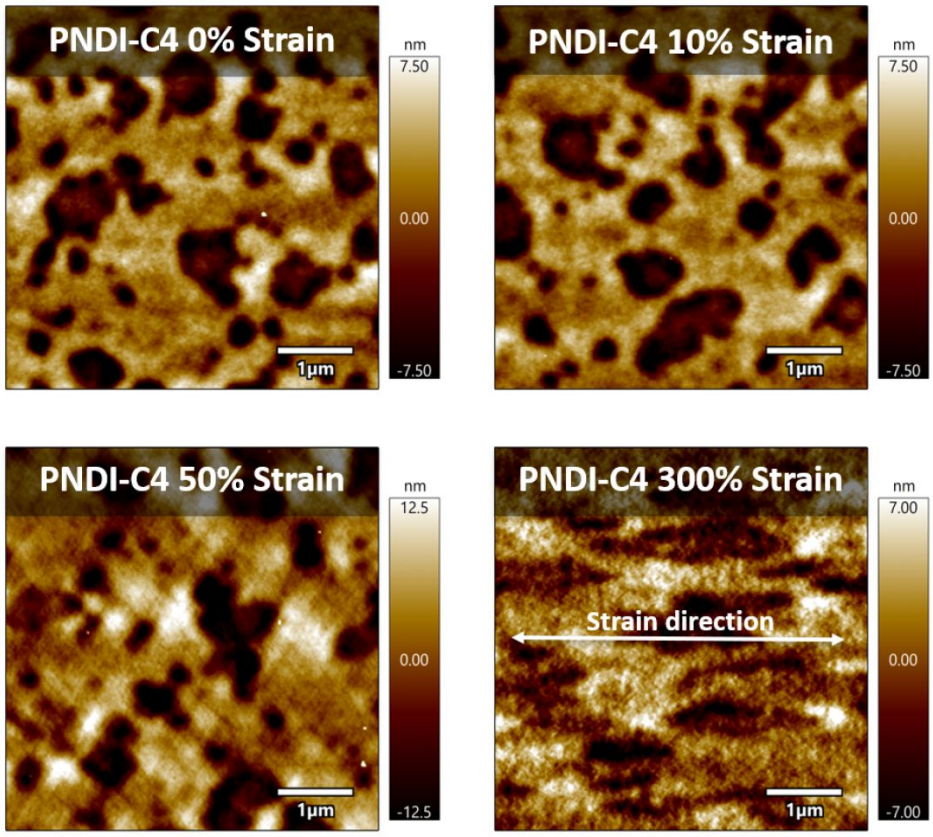


Figure S9: Atomic force microscopy of PNDI-C4 under tensile strain



Downloaded from pubs.acs.org/mamobx/article-supplement/508282/pdf/ma0c00889_si_001/ by PURDUE UNIV user on 28 October 2026

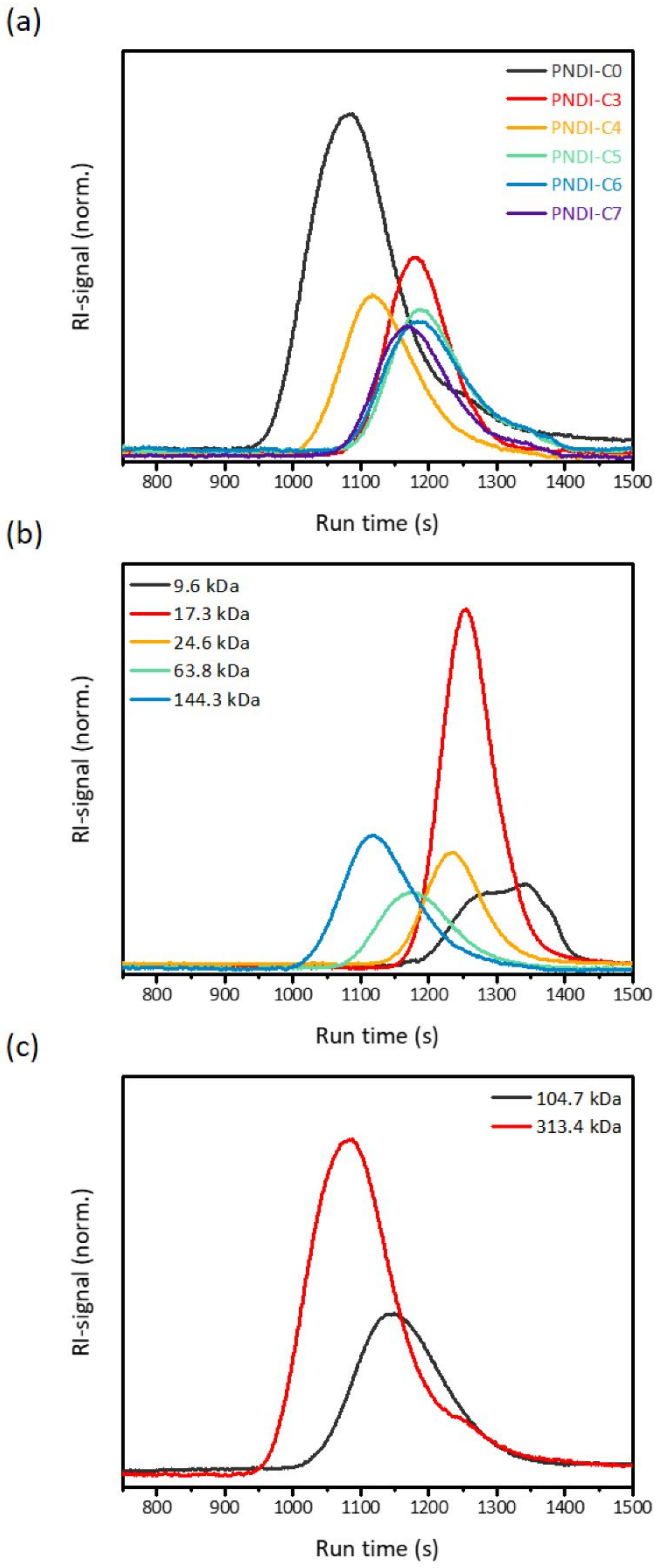


Figure S10: High-temperature size exclusion chromatography of PNDI polymers in 1,2,4-trichlorobenzene at 160 ˚C. a) SEC curves for all lengths of CBS incorporation. b) SEC curves of PNDI-C4 of varying molecular weight. c) SEC curves of PNDI-C0 of two molecular weights. All molecular weights shown are weight average molecular weight.



Downloaded from pubs.acs.org/mamobx/article-supplement/508282/pdf/ma0c00889_si_001/ by PURDUE UNIV user on 28 October 2026